

# Automated real-time cervical cancer diagnosis using NVIDIA Jetson Nano

Pallavi Mulmule<sup>1</sup>, Swati Shilaskar<sup>2</sup>, Shripad Bhatlawande<sup>2</sup>, Vedant Mulmule<sup>3</sup>, Vaishali H Kamble<sup>1</sup>,  
Jyoti Madake<sup>2</sup>

<sup>1</sup>Department of Electronics and Communication Engineering, School of Engineering and Technology, DES Pune University, Pune, India

<sup>2</sup>Department of Electronics and Telecommunication Engineering, Vishwakarma Institute of Technology, Pune, India

<sup>3</sup>Department of Information Technology, Vishwakarma Institute of Technology, Pune, India

## Article Info

### Article history:

Received Feb 27, 2025

Revised Aug 27, 2025

Accepted Sep 11, 2025

### Keywords:

Cervical cancer

Multi-layer perceptron

Pap smear

Real-time

Support vector machine

## ABSTRACT

Cervical cancer is a global health concern, making early detection critical for ensuring effective treatment outcomes. Screening technique, the Papanicolaou test (Pap test), has been adopted globally for timely detection. Nevertheless, the process of screening is subjective. The current study aims to advance the development of an automated real time framework for cervical cell analysis for early-stage diagnosis using supervised classification on NVIDIA Jetson Nano platform. Our approach, leveraging adaptive fuzzy k-means (AFKM) clustering and k-means clustering, extracts distinctive features from cervical cell images for accurate classification. Utilizing multilayer perceptron (MLP) and support vector machine (SVM) classifiers, we achieved a classification accuracy of 97%, highlighting the potential of our system for real-time applications in cervical cancer investigation. Validation by two expert pathologists further supports the system's practical utility.

*This is an open access article under the [CC BY-SA](https://creativecommons.org/licenses/by-sa/4.0/) license.*



## Corresponding Author:

Pallavi Mulmule

Department of Electronics and Communication Engineering, School of Engineering and Technology

DES Pune University

Pune, Maharashtra, India

Email: pallavi.mulmule@despu.edu.in

## 1. INTRODUCTION

Cancer has increasingly become a critical global health concern being the leading type among women across the globe. Furthermore, it is a major contributor to cancer-related mortality among women in developing regions, second to breast cancer. The study claims that the incidence of fatalities and occurrences in emerging nations (with poor and medium incomes) is higher than in developed nations. Identifying this cancer at an early stage is essential for addressing its impact effectively. In 2022, 14,100 new cases of cervical cancer were diagnosed, reported by American Cancer Society. Additionally, the illness lost the lives of some 4,280 female Americans [1]. According to cancer research [2], there are around 375,000 newly diagnosed cases of cancer reported in the UK each year or almost 1,000 cases per day. On the other hand, conditions in developing countries are terrible. 17% of all cancer-related fatalities in women are caused by cervical cancer. At the current incidence rates, 225,000 new cases are predicted to be reported annually in India by 2025 [3].

Human papillomavirus (HPV) is the leading factor responsible for the development of cervical cancer. In order to prevent such deadly diseases and to treat patients based on screening results, diagnosis at early stage is essential. The standard screening test for early examination and detection of cervical cancer in

the cervix is Papanicolaou test (Pap test). Developing a fully automated decision support system (DSS) based on Pap smear images with efficient identification of cervical dysplasia or precancerous changes is the main contribution of the current work. Automation-assisted screening techniques are being developed to decrease the cost of screening equipment, enhance the specificity and sensitivity of Pap smear screening and lessen the strain on cyto-technicians and cyto-pathologists, diagnosing cervical cancer early. The Pap smear investigation is now the utmost effective preventive method for early disease detection.

Literature reports use of machine vision techniques to analyse the characteristics of cytoplasm and nucleus which serves as a crucial biomarker for identification of disease. The majority of studies aimed at identifying cervical cancer make use of images from the Herlev dataset. Bora *et al.* [4] suggested use of support vector machine (SVM), k-nearest neighbours (KNN), Bayesian, ensemble technique and a maximum accuracy of 96.6% was claimed using the ensemble technique. For classification, Hemalatha and Rani [5] used neural networks and achieved the highest accuracy for multilayer perceptron (MLP) as 92%. For nucleus-level analysis, the adaptive nucleus shape modelling (ANSM) technique used Phoulady and Mouton [6] and reported cell categorisation by ANSM with a 93.33% accuracy rate. The deep neural network proposed Wang *et al.* [7], showed that the lightweight deep model outperforms conventional network and reported accuracy of 94.1%. Khamparia *et al.* [8] classified data using a variational autoencoder and a convolutional network. The outcomes show that diseases are classified at a higher classification rate of 97.89% using CNN's ResNet50 model. Hussain *et al.* [9] present deep convolutional neural network architectures: Resnet, Alexnet, Googlenet, VGGnet, and an ensemble approach. With 0.978 sensitivity, 0.979 specificity and 0.989 accuracy, the ensemble classifier outperformed. Mulmule and Kanphade [10] presented the work using MLP and SVM and predicted SVM outperformed over other for binary classification of cervical cell. Additionally, they conducted a study utilised novel two class classification approach for both segmentation and classification problem [11]. Table 1 provides a summary of the pertinent literature.

Table 1. Overview of relevant work

Author(s)	Classification model	Performance (%)
Athinarayanan and Srinath [12]	SVM, KNN, and ANN	Classification accuracy SVM-86, KNN-70, and ANN-65
Sharma <i>et al.</i> [13]	KNN	Classification accuracy of 84.3
Wu and Zhou [14]	SVM-PCA	Classification accuracy of 92
Bhargava <i>et al.</i> [15]	SVM, KNN, and ANN	Classification accuracy SVM-62, KNN-65, and ANN 95
Sompawong <i>et al.</i> [16]	Mask RCNN	Classification accuracy-89, sensitivity-72, and specificity 94
Xiang <i>et al.</i> [17]	YOLO+CNN	Sensitivity-97 and specificity-67
Shi <i>et al.</i> [18]	GCNN	Classification accuracy-95
Liu <i>et al.</i> [19]	CNN	Classification accuracy-91

The current work focuses machine vision techniques for identification and categorization of individual cells by leveraging unique characteristics of cell. Furthermore, the classification accuracy in several classification approaches was not up to par. Thus, the development of a reliable automated method for cervical cell identification and analysis is imperative. The following summarises the main features and contributions of the suggested system:

- The utilisation of unique feature set generation is completely unparalleled. It emphasises on development of a robust system leveraging advanced computer vision and artificial intelligence (AI) technologies to enhance decision-making processes.
- Our primary contribution lies in the development of an efficient and reliable abnormality detection system specifically optimized for deployment on the NVIDIA Jetson Nano board.
- By tailoring our solution to this platform, we achieve notable advantages over conventional methods, including improved scalability, accuracy, and processing speed. The system is designed to deliver high performance and low latency which makes it particularly best-suited for real-time applications.
- Experimental results demonstrate the superiority of our approach, highlighted by significantly reduced error rates and exceptional accuracy in real time, positioning it as a substantial advancement over existing techniques which will be definitely an aid tool for pathologist.

The following is the outline of the manuscript. Section 2 describes the conceptual framework of the suggested methodology. Section 3 describes results and discussion that goes along with them. The paper is finally concluded in section 4.

## 2. METHOD

The global database, which is openly accessible under a common creative license, is used in the suggested approach of detection [20]. The dataset incorporates 917 single-cell images as summerised in

Table 2, categorised into seven groups. Each image fits into one of the seven groups. We have used all 917 images for this investigation.

Table 2. Statistics of Herlev dataset

Primary class	Sub class	Count	Total
Normal	Superficial squamous	74	242
	Intermediate squamous	70	
	Columnar	98	
Cancerous	Mild dysplasia	182	675
	Moderate dysplasia	146	
	Severe dysplasia	197	
	Carcinoma in situ	150	

The workflow of suggested machine learning based system is displayed in Figure 1. The image has extraneous and unnecessary pixels. These pixels have a speckled noise-like appearance. Utilising contrast-limited adaptive histogram equalization (CLAHE), the speckle noise images are filtered. Second, the noise-filtered image is segmented using the adaptive fuzzy k-means (AFKM) segmentation method into foreground (i.e., nucleus-cytoplasm) and background. Thirdly, the complete dataset is then separated into training and validation set followed by feature extraction. Here, a total of forty features are extracted, taking into account the energy, entropy, colour, shape, size, intensity, orientation, and energy of the cytoplasm and nucleus separately. In next stage, all these 40 features are given to neural network and SVM with different kernels as an input. The MLP and SVM are trained with 70% image data and then tested with 30% image data. The complete process of training and testing is performed on the hardware platform Jetson Nano as represented in Figure 1.

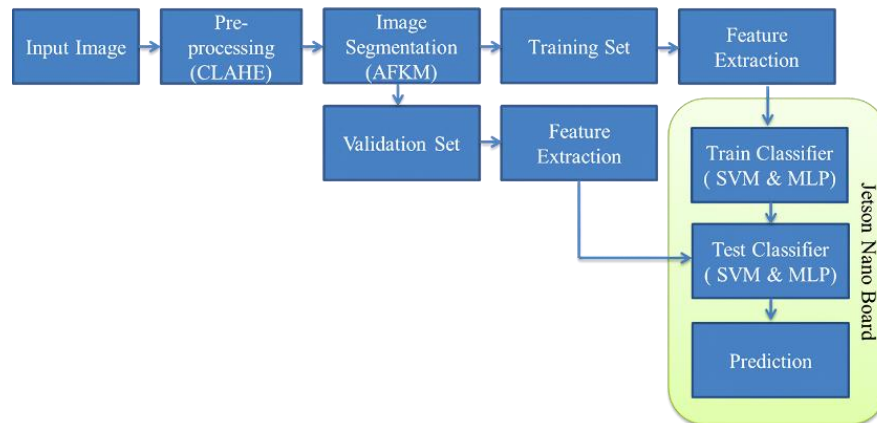


Figure 1. Proposed system for cervical cancer detection

## 2.1. Adaptive fuzzy k-means clustering

Above algorithm is a hybrid of fuzzy and classic k-means. In fuzzy k-means, each pixel is a member of two or more clustered groups. Let  $l(x,y)$  be the seed pixel under examination with clusters and cluster centre  $j$  and let  $I(x,y)$  be original image. Then new centre is computed using (1) [21]:

$$C_j = \frac{1}{m_{C_j}} \sum_{x \in C_j} \sum_{y \in C_j} l(x,y) \quad (1)$$

In k-means, the fuzzy technique is used to enable each pixel to simultaneously belong in many clusters with various degrees of membership. The membership function applied in this case is provided in (2):

$$m_{jp} = \frac{1}{\sum_{k=1}^{n_c} \left( \frac{d_{jp}}{d_{kp}} \right)^{2/(m-1)}} \quad (2)$$

where, distance  $d_{jp}$  is from p pixel to  $i^{\text{th}}$  current cluster centre,  $d_{kp}$  is distance from p pixel to  $j^{\text{th}}$  cluster centre, and m is fuzzy exponent. For better clustering, the degree of belongingness should be higher. The degree of belongingness  $B_j$  evaluates the centre's and its members' relative strength  $B_j = \frac{c_j}{m_{jp}}$ . The clustering process is improved by updating the membership degree and it is optimized on the basis of  $B_j$ . The optimization process is applied to ensure that the member is reassigned to its appropriate member cluster. However, there is possibility that largest fitness value member may also belong to smallest fitness value member which leads to miss-clustering. Therefore, member reassignment is done by putting constraint  $l(x, y) < c_{\text{larg}}$ , where  $c_{\text{larg}}$  is cluster with highest cluster value. The detailed explanation of AFKM can be found in [22].

## 2.2. Feature extraction

As previously mentioned, the clustering procedure segments the Pap smear images which consist of the cytoplasm and the cell nuclei. The next step involves extracting the properties of the cytoplasm and nucleus. Total 40 unique features are extracted from nucleus and cytoplasm which is explained further in detail.

Nucleus features: area, ratio of major and minor axis, diameter, ratio of short to long diameter, extent, eccentricity perimeter, elongation, position of nucleus, orientation, mean intensity in R, G, and B channel, contrast, correlation, variance, energy, entropy, and probability. Cytoplasm features: area, ratio of major and minor axis, diameter, ratio of short to long diameter, extent, eccentricity, C8 perimeter, C9 elongation, orientation, nucleus to cytoplasm ratio, mean intensity in R, G, and B channel, contrast, correlation, variance, energy, entropy, and probability.

## 2.3. Support vector machine

In order to more precisely separate data that cannot be separated linearly, supervised learning techniques called SVMs are used. The kernel function in SVM converts the pixel dimensions of the input cell into the feature space. The discriminant function is represented as (3):

$$g(X) = W^T \phi(X) + b \quad (3)$$

here, different kernel functions for classifying cells (i.e., normal and malignant) are considered, including linear, radial basis functions (RBF), 2nd and 3rd order polynomials. The nonlinear model known as the radial basis kernel function (RBF) in SVM is a linear estimator that maps n-dimensional input characteristics nonlinearly onto m-dimensional feature space. In (4) provides a mathematical expression for the model.

$$y = \sum_{j=1}^m w_j h_j(x) \quad (4)$$

In this case, y stands for the output class with uncertain weights w that change depending on the data. It's named hybrid RBF since the repressor is RBF with a Gaussian kernel. The m feature vector, also known as the basis functions, is used to create the non-linear mapping. Their centres in the input space and radius vector serve as characteristics for these basis functions [23].

## 2.4. Multilayer perceptron neural network

The traditional feed-forward multilayer perception neural network is composed of three layers. Hidden layer neurons are chosen using heuristic techniques. The sum of the products of the input signals and the connecting weights determines each of j neurons in hidden layer. The result is given in (5):

$$y = \sum_{j=1}^m w_j x_j \quad (5)$$

The back propagation network used here is based on the Levenberg–Marquardt (LM) algorithm [24]. Here, input layer contains 40 neurons (i.e., 40 features and 40 neurons) and output layer contains two neurons (i.e., two classes).

## 2.5. Model deployment on NVIDIA Jetson Nano platform

The NVIDIA Jetson Nano is compact and energy-efficient computing device designed for embedded systems and various other applications. It offers impressive computational capabilities, a quad-core ARM Cortex-A57 CPU, 128-core Maxwell GPU and NVIDIA Jetson platform. The device supports a range of interfaces and peripherals, including USB, ethernet, and HDMI [25]. Consuming only 5-10 watts on

average, the Jetson Nano is an ideal solution for edge computing. Furthermore, its 25.6 GB/s memory bandwidth ensures rapid and efficient data transfer between the CPU and GPU.

All these features enable the hardware to perform complex computations at low power consumption, making it a good platform to execute deep learning models. In addition, it has ample space for managing big datasets and deep learning models with LPDDR4 memory of 4 GB. With every aspect considered, NVIDIA Jetson Nano is a great option for implementing cutting edge AI solutions due to its low power consumption and memory bandwidth parameters. The NVIDIA Jetson Nano supports major deep learning frameworks such as TensorFlow, PyTorch, and ONNX making it versatile for various AI applications. It leverages NVIDIA CUDA, cuDNN, and TensorRT to enable GPU acceleration, ensuring efficient processing of complex computations. Additionally, TensorRT provides optimized inference capabilities with support for FP16 and INT8 precision, significantly reducing latency and enhancing real-time performance.

Setup for image classification:

- a. Hardware: Nano board connected to a Power supply via a 5V barrel jack or Micro-USB.
- b. Software: JetPack SDK (includes Ubuntu-based OS, CUDA, cuDNN, and TensorRT).
- c. Workflow:
  - 1) Prepare the model:
    - Select or train a model: train an image classification model using frameworks like TensorFlow, PyTorch, or ONNX.
    - Optimize the model: convert the model to a lightweight format like TensorFlow Lite, ONNX, or NVIDIA TensorRT for better performance on edge devices.
  - 2) Set up the hardware
    - Install operating system: flash the appropriate OS on an SD card. For Jetson Nano use NVIDIA JetPack SDK.
    - Boot and configure: boot the device and configure it. Also install dependencies.
    - Transfer and test model: transfer the model file to the device using SCP, USB, and write deployment code. Finally test the performance of model.

The trained model was initially converted to the ONNX format for cross-platform interoperability before being further optimised with NVIDIA TensorRT to allow for real-time processing on Jetson Nano. The Jetson Nano's CUDA cores are fully utilised by TensorRT, a high-performance inference engine made especially for NVIDIA GPUs. It speeds up model inference through the use of layer fusion, GPU kernel optimisations and precision calibration. The popular frameworks for deploying machine learning models on edge devices include TensorFlow Lite, ONNX, and TensorRT. While ONNX facilitates simple cross-platform interoperability, TensorRT offers the best performance on NVIDIA hardware through sophisticated GPU optimisations, and TensorFlow Lite offers lightweight model conversion and quantisation, mainly for mobile and embedded CPUs. The suggested system is well-suited for point-of-care cervical cancer screening since it significantly lowers inference latency when deployed on edge hardware such as the Jetson Nano, safeguards patient data privacy by avoiding cloud uploads, and guarantees accurate real-time classification even in low-connectivity environments.

### 3. RESULTS AND DISCUSSION

Initially, cervical images are pre-processed using contrast enhancement by CLAHE, as mentioned earlier. The CLAHE is a local contrast enhancement technique designed to increase image's contrast. CLAHE increases an image's brightness, which facilitates finding visual details. Figure 2 displays the enhanced image after applying contrast enhancement.

By comparing the original image with the CLAHE-processed image, as shown in Figures 2(a) and (b), it is evident that Figure 2(b) demonstrates significant enhancement in contrast and sharpening of visual details. This improvement has a substantial effect on the segmentation results. Prior to applying CLAHE, the boundaries between regions are indistinct, leading to imprecise and poorly defined segmentation outputs.

#### 3.1. Result of cell segmentation stage

Initially, the regions were clustered using AFKM segmentation and k-means clustering. Figure 3 demonstrates the region of interest (ROI) extraction results using two different clustering algorithms: k-means clustering and AFKM. Figure 3(a) shows the original input microscopic images of cells. Figure 3(b) depicts the segmentation output using standard k-means clustering. Figure 3(c) displays the pseudo-colour depiction of the segmented regions for better visibility. Figure 3(d) illustrates the segmentation result using the AFKM algorithm.

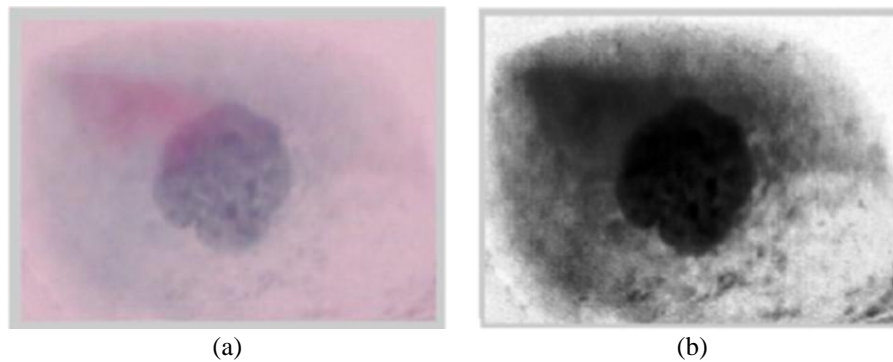


Figure 2. Pre-processing using CLAHE; (a) input image and (b) output image

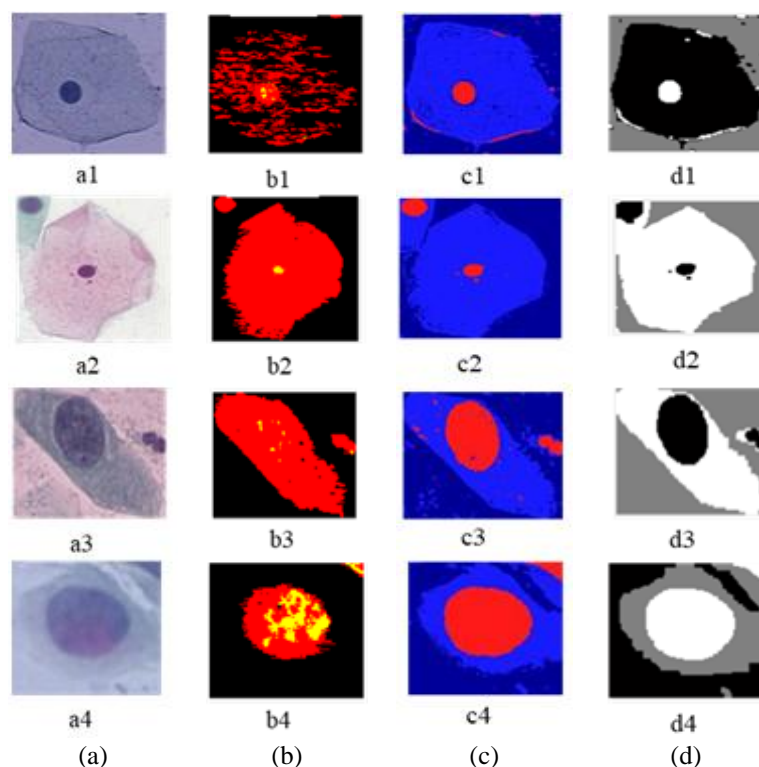


Figure 3. ROI extractions by k-means clustering and AFKM algorithm; (a) input image, (b) k-means clustering output, (c) pseudo colour output image, and (d) AFKM output

Significant noise and over-segmentation can be seen in the segmentation results of conventional k-means clustering. Although the regions of interest (nuclei/cells) are partially retrieved, in a number of instances (e.g., b2 and b4), the boundaries are irregular and non-uniform. False positives and background artefacts are also noticeable, particularly in areas with low contrast or complexity. Different colours are used to highlight the segmented areas in the pseudo-color representations. The primary advantage is that it improves the segmented sections' visual interpretability. When compared to k-means, the AFKM segmentation results (d1–d4) show better performance. The boundaries of the ROI are more consistent, smoother, and appear more like actual cell architectures.

The algorithm adapts better to variations in intensity and texture, effectively reducing noise and irrelevant regions. It is evident that AFKM method performs noticeably better than the conventional k-means clustering. The AFKM method reduces erroneous segmentation, manages intensity inhomogeneities better and offers boundaries that are clearer and more accurate. The accuracy of automated diagnostic systems is eventually increased by this better segmentation quality which is essential for later analytical stages like feature extraction and classification.

Feature extraction: segmented sections of the cytoplasm and nucleus yielded a total of 40 morphological, textural and intensity-based characteristics. AFKM, which produces a binary mask to precisely localise nucleus borders, was used for the segmentation. Using the AFKM mask exclusively to separate the regions of interest, feature extraction was performed on the original RGB Pap smear image. The masked areas that corresponded to the cytoplasm and nucleus were used to calculate colour attributes including mean intensity in red, green, and blue channels. Likewise, the segmented binary masks were used to compute spatial parameters such as area, eccentricity, elongation, and axis ratios. Utilising gray-level co-occurrence matrix (GLCM) statistics applied to the original image pixels within the segmented regions, texture properties such as contrast, correlation, energy, and entropy were extracted. Ultimately, the classifiers are trained using these attributes.

### 3.2. Results of cell classification

A total of 917 images from the Herlev dataset were used for the performance evaluation of the system. The MLP and SVM are trained with 70% image data and then tested with 30% image data. The performance of two classifiers MLP and SVM for two classes, (i.e., normal and cancerous) is analysed on the hardware platform. Figure 4 shows the complete setup and testing result on the terminal respectively. Figure 4(a) shows a complete embedded development setup built around the NVIDIA Jetson Nano single-board computer. It interfaces with a monitor displaying a Linux-based GUI, where file system directories are visible, indicating the system is up and running. Figure 4(b) illustrates how to run a shell script for image classification and compile a source file using OpenCV libraries. The script returns categorisation results after processing samples of normal and malignant images. This demonstrates the practical implementation and testing of the proposed method for automated biomedical image analysis.

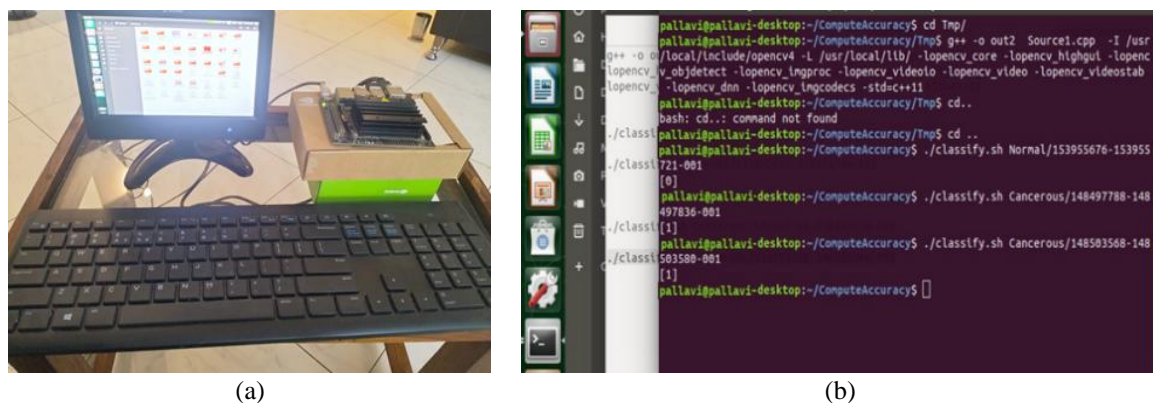


Figure 4. System implementation and testing; (a) hardware setup using NVIDIA Jetson Nano and (b) terminal output showing classification results

In the current work, SVM and MLP are the two classifiers employed with 10-fold cross-validation. Nine performance indices—accuracy, sensitivity, specificity, precision, F1-score, Matthews correlation coefficient (MCC), positive and negative predictive values, and kappa score—are used for performance evaluation of two frameworks. The total time required to test a single image on hardware is 2.682 seconds while 425 milliseconds on a machine (quad core 2.6 GHz processor with graphics card). For seven sub-classes, Table 3 summarizes performance analysis of classifiers for various kernel functions.

Table 3. Comparison of the SVM and MLP classification techniques

Classifier and kernel function	Sen.	Spc.	Pre.	NPV	PPV	F1-score	MCC	Acc.	Kappa score
SVM: linear	93	90	87	97	89	93	87	88	86
SVM: 2 order polynomial	96	99	99	96	99	97	95	96	95
SVM: 3 order polynomial	92	99	99	92	99	96	91	94	91
MLP: RBF	92	98	98	92	98	95	90	95	90
MLP: Tan h	97	92	92	98	93	95	90	97	90
MLP: rectified linear unit (ReLu)	94	96	97	93	97	95	90	94	90
MLP: Sigmoid	92	97	97	92	97	94	89	93	89



### 3.3. Discussion

Hand-crafted morphological, intensity, and textural features taken from AFKM-segmented nucleus and cytoplasm regions are used in the suggested framework. This makes it ideal for real-time deployment on the Jetson Nano since it guarantees interpretability, minimal computational cost, and dependable performance on a small number of biomedical datasets. On the other hand, lightweight CNNs like MobileNetV3 and quantised YOLOv5n can learn features directly from images and have good accuracy, but they usually need more processing power and big annotated datasets. Therefore, interpretability and efficiency are given priority in our method, and future research may incorporate CNN-based descriptors into hybrid models to improve robustness.

Table 3 discusses the nine performance parameters used to evaluate the two classifiers being considered. The average of every result obtained using the 10-fold cross validation method is applied across all folds. Table 3 demonstrates that hyperbolic tangent activation function-based MLP classifier performs better than the sigmoid and ReLu activation functions for every performance criterion. Additionally, the SVM classifier is evaluated for four kernel functions. It was found that, for all evaluation criteria, the second order polynomial kernel outperformed the other three SVM kernel functions. SVM classifier with second order polynomial function and MLP classifier with the hyperbolic tangent as activation function were outperformed.

Using an MLP classifier with Tan h activation function, the maximum sensitivity of 97%, accuracy of 97%, specificity of 92%, positive predictive value of 93%, and F1 score of 95% were recorded. A second order polynomial for SVM came out with a maximum accuracy of 96% and a kappa score of 95%. MLP had a higher sensitivity and accuracy, which are often critical for cancer detection. The performance analysis of all the evaluation metrics is presented in graphical format in Figure 5. From Figure 6, it is evident that, SVM (2nd-order polynomial) achieved the highest AUC (0.97), followed by several MLP variants. The performance metrics are also compared to the most recent documented literature, as shown in Table 4. Evidently, the hyperbolic tangent activation function of MLP and the second order polynomial of SVM provide superior performance.

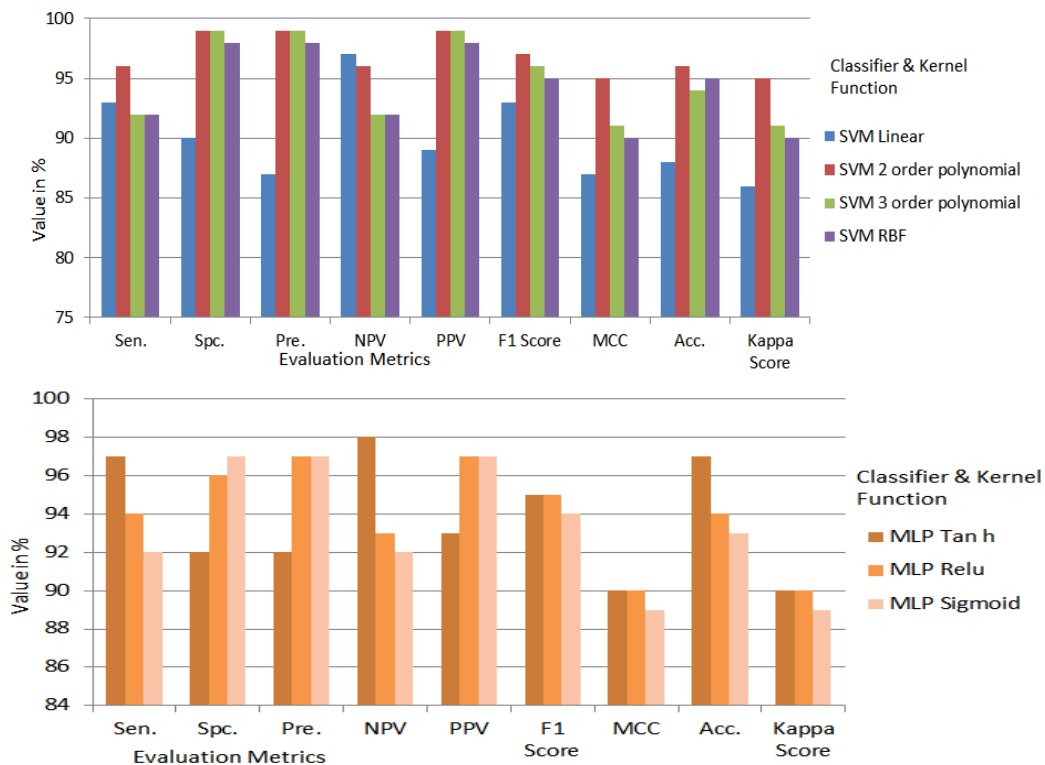


Figure 5. Performance analysis of SVM and MLP classifier for various kernel functions



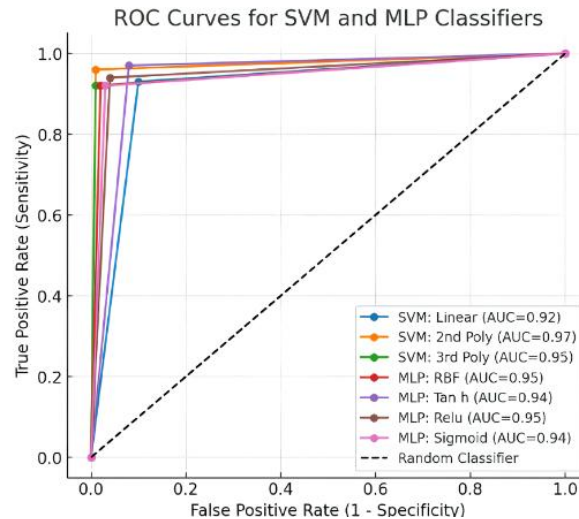


Figure 6. ROC-AUC plot for SVM and MLP classifiers with various kernel functions

Table 4. Performance comparison with state of art literature

Source	Classifier	Accuracy (%)	Sensitivity (%)	Specificity (%)
Hemalatha and Rani [5]	MLP, PNN, and LVQ	MLP-92.03	MLP-78.09	MLP-90.43
		PNN-26.99	PNN-100	PNN-26.39
		LVQ-83.42	LVQ-99.25	LVQ-82
Bora <i>et al.</i> [4]	Ensemble	96.51	96.88	89.67
Devi and Thirumurugan [26]	KNN	96.28	97.96	83.65
Wang <i>et al.</i> [27]	SVM	96	-	-
Kudva <i>et al.</i> [28]	Hybrid-Alexnet and VGG	91.46	-	-
Kashyap <i>et al.</i> [29]	SVM	95	-	-
Proposed method	MLP tan <i>h</i> activation function	97	97	92

#### 4. CONCLUSION

In this work, an automated cervical cancer detection and classification framework capable of accurately identifying and segmenting cell nuclei in microscopic Pap smear images was presented. The suggested system demonstrated a fast and efficient feature extraction method that surpasses traditional techniques by introducing a unique set of statistical shape, intensity, and colour features to analyse nucleus chromatin patterns. The system's supervised classification approach, using an SVM classifier with a second-order polynomial and an MLP classifier with a hyperbolic tangent activation function, achieved significant improvements in classification accuracy, sensitivity, and specificity.

A key contribution of this work is its successful implementation on the NVIDIA Jetson Nano platform, enabling real-time processing capabilities in a resource-constrained embedded environment. Comparative analysis with existing methods in the literature confirms that our methodology is robust and precise. The feature extraction outputs, including nucleus segmentation masks and chromatin descriptors, were validated by comparing them with expert annotations from two pathologists. Validation by two expert pathologists further supports the system's practical utility in distinguishing normal and malignant cervical cells with high reliability. However, the current framework has been evaluated on a specific dataset and requires further validation using larger and more diverse Pap smear image datasets to ensure its generalizability across different population groups and clinical settings. Additionally, although the system has been successfully implemented on the NVIDIA Jetson Nano for real-time processing, further analysis can be done to fully assess and optimize its computational efficiency, especially for deployment on other low-power edge computing devices.

Future research should focus on developing hybrid models that combine multiple classifiers or integrate deep learning approaches to enhance detection performance. Overall, this research contributes a practical, accurate, and efficient tool that supports early cervical cancer detection, aiming to improve patient care and enable timely treatment interventions.

#### FUNDING INFORMATION

Authors state no funding involved.

## AUTHOR CONTRIBUTIONS STATEMENT

This journal uses the Contributor Roles Taxonomy (CRediT) to recognize individual author contributions, reduce authorship disputes, and facilitate collaboration.

Name of Author	C	M	So	Va	Fo	I	R	D	O	E	Vi	Su	P	Fu
Pallavi Mulmule	✓	✓	✓	✓	✓	✓	✓	✓	✓				✓	
Swati Shilaskar	✓		✓		✓	✓			✓		✓	✓		
Shripad Bhatlawande		✓		✓		✓	✓	✓		✓		✓	✓	
Vedant Mulmule		✓	✓		✓		✓	✓	✓	✓	✓			
Vaishali H Kamble		✓		✓	✓		✓	✓		✓	✓	✓	✓	
Jyoti Madake		✓	✓			✓		✓		✓	✓			

C : **C**onceptualization

M : **M**ethodology

So : **S**oftware

Va : **V**alidation

Fo : **F**ormal analysis

I : **I**nterpretation

R : **R**esources

D : **D**ata Curation

O : **O**riginal Draft

E : **E**diting

Vi : **V**isualization

Su : **S**upervision

P : **P**roject administration

Fu : **F**unding acquisition

## CONFLICT OF INTEREST STATEMENT

Authors state no conflict of interest

## DATA AVAILABILITY

Data availability is not applicable to this paper as no new data were created or analyzed in this study.




## REFERENCES

- [1] National Cancer Institute, "Cancer Statistics Facts: Cervical Cancer," *SEER Cancer Statistics, National Cancer Institute*. [Online]. Available: <https://seer.cancer.gov/statfacts/html/cervix.html>. (Date accessed: Dec. 14, 2023).
- [2] Cancer Research UK, "Cervical cancer statistics," *Technical Report*, 2019. [Online]. Available: <https://www.cancerresearchuk.org/health-professional/cancer-statistics/statistics-by-cancer-type/cervical-cancer>. (Date accessed: Dec. 17, 2023).
- [3] R. Mehrotra and K. Yadav, "Cervical Cancer: Formulation and Implementation of Govt of India Guidelines for Screening and Management," *Indian Journal of Gynecologic Oncology*, vol. 20, no. 1, p. 4, Mar. 2022, doi: 10.1007/s40944-021-00602-z.
- [4] K. Bora, M. Chowdhury, L. B. Mahanta, M. K. Kundu, and A. K. Das, "Automated classification of Pap smear images to detect cervical dysplasia," *Computer Methods and Programs in Biomedicine*, vol. 138, pp. 31–47, Jan. 2017, doi: 10.1016/j.cmpb.2016.10.001.
- [5] K. Hemalatha and K. U. Rani, "An Optimal Neural Network Classifier for Cervical Pap Smear Data," in *Proceedings - 7th IEEE International Advanced Computing Conference, IACC 2017*, Jan. 2017, pp. 110–114, doi: 10.1109/IACC.2017.0036.
- [6] H. A. Phoulady and P. R. Mouton, "A New Cervical Cytology Dataset for Nucleus Detection and Image Classification (Cervix93) and Methods for Cervical Nucleus Detection," *arXiv*, 2018, doi: 10.48550/arXiv.1811.09651.
- [7] H. Wang, C. Jiang, K. Bao, and C. Xu, "Recognition and Clinical Diagnosis of Cervical Cancer Cells Based on our Improved Lightweight Deep Network for Pathological Image," *Journal of Medical Systems*, vol. 43, no. 9, p. 301, Sep. 2019, doi: 10.1007/s10916-019-1426-y.
- [8] A. Khamparia, D. Gupta, J. J. P. C. Rodrigues, and V. H. C. de Albuquerque, "DCAVN: Cervical cancer prediction and classification using deep convolutional and variational autoencoder network," *Multimedia Tools and Applications*, vol. 80, no. 20, pp. 30399–30415, Aug. 2021, doi: 10.1007/s11042-020-09607-w.
- [9] E. Hussain, L. B. Mahanta, C. R. Das, and R. K. Talukdar, "A comprehensive study on the multi-class cervical cancer diagnostic prediction on pap smear images using a fusion-based decision from ensemble deep convolutional neural network," *Tissue and Cell*, vol. 65, p. 101347, Aug. 2020, doi: 10.1016/j.tice.2020.101347.
- [10] P. V. Mulmule and R. D. Kanphade, "Supervised classification approach for cervical cancer detection using Pap smear images," *International Journal of Medical Engineering and Informatics*, vol. 14, no. 4, pp. 358–368, 2022, doi: 10.1504/IJMEI.2022.123930.
- [11] P. V. Mulmule, R. D. Kanphade, and D. M. Dhane, "Artificial intelligence-assisted cervical dysplasia detection using papanicolaou smear images," *Visual Computer*, vol. 39, no. 6, pp. 2381–2392, Jun. 2023, doi: 10.1007/s00371-022-02463-9.
- [12] S. Athinayanan and M. V. Srinath, "Classification of Cervical Cancer Cells in Pap Smear Screening Test," *ICTACT Journal on Image and Video Processing*, vol. 6, no. 4, pp. 1234–1238, May 2016, doi: 10.21917/ijivp.2016.0179.
- [13] M. Sharma, S. K. Singh, P. Agrawal, and V. Madaan, "Classification of Cervical Cancer using KNN," *Indian Journal of Science and Technology*, vol. 9, no. 28, Jul. 2016, doi: 10.17485/ijst/2016/v9i28/98380.
- [14] W. Wu and H. Zhou, "Data-driven diagnosis of cervical cancer with support vector machine-based approaches," *IEEE Access*, vol. 5, pp. 25189–25195, 2017, doi: 10.1109/ACCESS.2017.2763984.
- [15] A. Bhargava, P. Gairola, G. Vyas, and A. Bhan, "Computer Aided Diagnosis of Cervical Cancer Using HOG Features and Multi Classifiers," in *Advances in Intelligent Systems and Computing*, vol. 624, 2018, pp. 1491–1502, doi: 10.1007/978-981-10-5903-2\_155.
- [16] N. Sompawong et al., "Automated Pap Smear Cervical Cancer Screening Using Deep Learning," in *Proceedings of the Annual International Conference of the IEEE Engineering in Medicine and Biology Society, EMBS*, Jul. 2019, pp. 7044–7048, doi: 10.1109/EMBS.2019.8856369.




- [17] Y. Xiang, W. Sun, C. Pan, M. Yan, Z. Yin, and Y. Liang, "A novel automation-assisted cervical cancer reading method based on convolutional neural network," *Biocybernetics and Biomedical Engineering*, vol. 40, no. 2, pp. 611–623, Apr. 2020, doi: 10.1016/j.bbe.2020.01.016.
- [18] J. Shi, R. Wang, Y. Zheng, Z. Jiang, H. Zhang, and L. Yu, "Cervical cell classification with graph convolutional network," *Computer Methods and Programs in Biomedicine*, vol. 198, p. 105807, Jan. 2021, doi: 10.1016/j.cmpb.2020.105807.
- [19] W. Liu *et al.*, "CVM-Cervix: A hybrid cervical Pap-smear image classification framework using CNN, visual transformer and multilayer perceptron," *Pattern Recognition*, vol. 130, p. 108829, Oct. 2022, doi: 10.1016/j.patcog.2022.108829.
- [20] MDE-Lab, "PAP-SMEAR (DTU/HERLEV) DATABASES & RELATED STUDIES." [Online]. Available: <http://mde-lab.aegean.gr/index.php/downloads/>. (Date accessed: Dec. 21, 2018).
- [21] M. Y. Mashor, "Hybrid Training Algorithm for RBF Network," *International Journal of the Computer, The Internet and Management*, vol. 8, no. 1990, pp. 50–65, 2000.
- [22] N. A. M. Isa, S. A. Salamah, and U. K. Ngah, "Adaptive fuzzy moving k-means clustering algorithm for image segmentation," *IEEE Transactions on Consumer Electronics*, vol. 55, no. 4, pp. 2145–2153, Nov. 2009, doi: 10.1109/TCE.2009.5373781.
- [23] T. Poggio and F. Girosi, "Regularization Algorithms for Learning That Are Equivalent to Multilayer Networks," *Science*, vol. 247, no. 4945, pp. 978–982, Feb. 1990, doi: 10.1126/science.247.4945.978.
- [24] S. N. Oğulata, C. Şahin, and R. Erol, "Neural network-based computer-aided diagnosis in classification of primary generalized epilepsy by EEG signals," *Journal of Medical Systems*, vol. 33, no. 2, pp. 107–112, Apr. 2009, doi: 10.1007/s10916-008-9170-8.
- [25] N. Corporation, "Jetson Nano Module," *NVIDIA Developer*. [Online]. Available: <https://developer.nvidia.com/embedded/jetson-nano>. (Date accessed: Feb 21, 2024).
- [26] N. L. Devi and P. Thirumurugan, "Cervical Cancer Classification from Pap Smear Images Using Modified Fuzzy C Means, PCA, and KNN," *IETE Journal of Research*, vol. 68, no. 3, pp. 1591–1598, May 2022, doi: 10.1080/03772063.2021.1997353.
- [27] P. Wang, L. Wang, Y. Li, Q. Song, S. Lv, and X. Hu, "Automatic cell nuclei segmentation and classification of cervical Pap smear images," *Biomedical Signal Processing and Control*, vol. 48, pp. 93–103, Feb. 2019, doi: 10.1016/j.bspc.2018.09.008.
- [28] V. Kudva, K. Prasad, and S. Guruvare, "Hybrid Transfer Learning for Classification of Uterine Cervix Images for Cervical Cancer Screening," *Journal of Digital Imaging*, vol. 33, no. 3, pp. 619–631, Jun. 2020, doi: 10.1007/s10278-019-00269-1.
- [29] D. Kashyap *et al.*, "Cervical cancer detection and classification using Independent Level sets and multi SVMs," in *2016 39th International Conference on Telecommunications and Signal Processing, TSP 2016*, Jun. 2016, pp. 523–528, doi: 10.1109/TSP.2016.7760935.

## BIOGRAPHIES OF AUTHORS






**Pallavi Mulmule**    received Ph.D. degree from Savitribai Phule Pune University, Pune, India. She has published nineteen research articles in international and national journals and conferences. Her research interests include digital image processing, biomedical engineering, embedded systems, and digital electronics. She holds one copyright and three patents. She has 20 years of teaching and research experience in the field of image processing, IoT, and digital electronics. She can be contacted at email: [pallavi.mulmule@despu.edu.in](mailto:pallavi.mulmule@despu.edu.in).






**Swati Shilaskar**    pursued Ph.D. from Government College of Engineering Amravati. She received the B.E. degree in electronics engineering, the M.E. degree in digital electronics from Sant Gadge Baba Amravati University, India. Her research interests include BCI, medical diagnostic support systems, and automation. She can be contacted at email: [swati.shilaskar@vit.edu](mailto:swati.shilaskar@vit.edu).






**Shripad Bhatlawande**    received Ph.D. degree from the Indian Institute of Technology Kharagpur, India, in 2015. He received bachelor's degree in Electronics Engineering from the SGGS COE, Nanded, India, in 2000 and Master's degree in Electronics Engineering from the Government College of Engineering, Pune, India, in 2008. His research interests include embedded systems, machine intelligence, and robotics. He can be contacted at email: [shripad.bhatlawande@vit.edu](mailto:shripad.bhatlawande@vit.edu).






**Vedant Mulmule**    is a research scholar and a graduate student in the Information Technology Department at BRAC's Vishwakarma Institute of Technology, Pune. His areas of interest include data structures, computer vision, artificial intelligence, data science, and microprocessors. He can be contacted at email: vedant.mulmule23@vit.edu.



**Vaishali H Kamble**    is currently working in DES Pune University as Assistant Professor. She holds a Ph.D. degree in Electronics and Telecommunication from Savitribai Phule Pune University, Pune, India. She was a Women Research Scientist of the Department of Science and Technology, New Delhi. She is a fellow member of IETE and IEEE. Her research areas are image processing, computer vision, machine learning, deep learning, and communication systems. She can be contacted at email: vaishaliraichurkar@gmail.com.



**Jyoti Madake**    received Ph.D. degree from Savitribai Phule University, Pune, India. She received Bachelor's degree in Electronics Engineering from Sardar Patel College of Engineering, Mumbai, India and Master's degree in Microelectronics from Birla Institute of Technology, Pune. Her research interests include machine learning, embedded systems, and deep learning. She can be contacted at email: jyoti.madake@vit.edu.